The thermal expansion properties of halogen bond containing 1-4 dioxane halogen complexes.

W. G. Marshall,[a‡] R. H. Jones[b*] and K. S. Knight[c,d]

[a]ISIS Facility, STFC Rutherford Appleton Lab, Harwell Oxford, Didcot OX11 0QX, Oxon, United Kingdom.

[b]School of Chemical and Physical Sciences, Keele University, Keele, ST5 5BG, United Kingdom. Fax 44 1792 712378, Tel: 44 1782 733033,

[c]Department of Earth Sciences, University College London, Gower Street, London, WC1E 6BT, United Kingdom.,

[d]Department of Earth Sciences, The Natural History Museum, Cromwell Road, London, SW7 5BD United Kingdom.

[‡] Deceased.

- Correspondence e-mail r.h.jones@keele.ac.uk

Abstract

Neutron powder diffraction has been used to determine accurate molecular structures and thermal expansion properties for the complexes formed between by iodine and bromine with 1,4 dioxane. The marked anisotropy in the magnitudes of the principal axes of the thermal expansion tensor for both compounds can be associated with the different intermolecular forces present, with the smallest values being associated with the halogen bonds formed between oxygen and the diatomic halogen molecules. The smallest thermal expansion coefficient of the 1,4 dioxane iodine complex is smaller than the corresponding coefficient in the corresponding bromine complex reflecting the stronger halogen bond formed between iodine and oxygen when compared to that formed between oxygen and bromine.

Background

The study of halogen bonded complexes continues to be a growth area in chemistry, and an operational definition has been assigned to the halogen bond by IUPAC namely “A halogen bond occurs when there is evidence of a net attractive interaction between an electrophilic region associated with a halogen atom in a molecular entity and a nucleophilic region in another, or the same,

molecular entity[1]". When halogen bonded interactions were extensively studied in solution during the 1950s, the intermolecular bonding present in these interactions was believed to be based on the donation of a pair of electrons from the donor molecule (lone pair or π orbital) into the σ^* anti bonding orbital of the acceptor molecule. This view was based on the then accepted view of bonding in charge transfer complexes[2]. By contrast, the current view of bonding in halogen bonded complexes (which is currently the most widely accepted) emphasizes an electrostatic interaction involving a region of negative potential on the donor, and an area of positive potential on the halogen, the so-called σ-hole[3,4,5]. This model with the inclusion of polarization and dispersion effects[6,7], has become the accepted model of bonding in most halogen bonded complexes[8]. The growth in interest in halogen bonding is no doubt a consequence of their role over a wide variety of areas of chemistry. Some of these are well known and long established, for example in supramolecular chemistry[9,10,11], crystal engineering[3,12] liquid crystals[13,14,15], and biological systems[16], with the best-known example of the latter being the long established role of iodine in thyroid hormones[17]. These, and other areas, have been the subject of a recent major review[18]. One aspect which has received relatively less attention is that of their thermal expansion properties. There are several reasons why the properties of halogen bonds with temperature should be investigated. The first which we alluded to in the introduction in that observing changes that occur in a halogen bond as a function of temperature will enable further refinements /improvements to the theoretical description of halogen bonding. Initial studies on systems containing Ar-I ···N, Ar-I ···O, and Ar-Br ···N moieties (Ar = perfluorinated unit) revealed that there were significant changes in the donor (donor = N, O)··· halogen distances with temperature, with the donor·· halogen distances decreasing with decreasing temperature[19]. Second, some examples on the thermal expansion properties of systems containing halogen bonds show unusual results. For example, colossal thermal expansion was recently observed in co-crystals formed from azo bipyridine with 4,6 halogenated resorcinols[20]. Other studies on strong halogen bonds involving dihalogen molecules as the acceptor have also revealed colossal thermal expansion[21], together with the rarer phenomena of negative area expansion[22]. Thirdly, halogen bonds come in different "varieties", compared to hydrogen bonds (more than one halogen) and as a consequence it is pertinent to ask if their expansion properties differ, and how they compare with other intermolecular forces that are present, and it is this last question that we shall address in the study by comparing the expansion properties of the isostructural halogen bonded complexes formed between 1,4-dioxane and bromine and iodine.

By their nature thermal expansion properties of solids can be measured directly by methods such as dilatometry[23], but are more often investigated by diffraction based techniques which measures the changes in the size of the unit cell metric and hence probes directional expansion as the

temperature is altered[24]. If these individual diffraction measurements are of sufficient quality to permit structural refinement, it is possible to obtain accurate measurements of the interatomic contacts and angles of the molecules, and how these also respond to the variation in temperature. Whilst many of these measurements have made use of single crystal diffraction[25], powder-based methods offer certain well-known advantages. For example, powder diffractometers are not subject to centring errors, and generally offer higher real-space resolution. The material is sampled in as the bulk, whilst an individual crystal might be atypical. Powder diffraction eliminates the problems associated with twinning, or even the crystal shattering, which may occur if the material undergoes a first order phase transition for example as seen in pyrene[26]. In addition, it has been demonstrated that the data collected using high resolution neutron diffraction can yield structural information which is comparable to that collected with single crystal measurements, for example acetone[27]; pyridine[28] metsitylene[29],.Thus high resolution neutron powder diffraction offers a reliable way of extracting structural information as the environment of the sample is changed.

Because of the relatively few studies that have been carried out to investigate the thermal expansion properties of systems containing halogen bonds, we considered a systematic study of a series of such systems would enable information on how changes within these structures caused by the variation of temperature could affect the macroscopic expansion properties. Furthermore, there have been very few studies on halogen bonded systems using neutron diffraction[22,23,30, 31], Indeed, none were referenced in the recent comprehensive review on halogen bonding [18]. As mentioned earlier, neutron powder diffraction has been successfully used to obtain high quality structures in the which the accuracy of structural parameters is comparable to single crystal studies. An additional advantage of using neutron diffraction is that accurate hydrogen (deuterium for powder diffraction studies) positions can be obtained. This is because the diffracted intensities are not dominated by the presence of heavy elements with large number of electrons as in the case of X-ray scattering, but since the neutron scattering lengths are a nuclear property, all elements and their isotopes are found to have approximately comparable magnitudes, and hence they contribute equally to the diffraction pattern. For example, in the structure of $(CH_3)_3N\cdots ICl$, we were able to show that significant changes could be seen in the geometry involving the hydrogen atoms of the$(CH_3)_3N$ moiety in the complex, when compared to that of the free molecule. These changes, which occurred upon complexation, could not be unambiguously observed when the crystal structure was determined by X-ray diffraction. In addition to these changes, we could explicitly show the existence of weak C-H···Y hydrogen bonds[31]. Furthermore, in the N···I-Cl moiety, the ability of the chlorine atom to act as the acceptor in a weak C-H···Cl hydrogen bounds appeared to be enhanced upon complex formation, and that the hydrogen

atom occupied a well-defined position at approximately 90° relative to the internuclear axis of the ICl molecule.

We have chosen to study systems based on the complexes formed between diatomic halogen molecules and 1-4, dioxane. These were some of the first halogen bonded complexes to have had their crystal structures determined[32,33]. The molecular structures of the complexes utilising chlorine and bromine were determined in the 1950s and the iodine analogue more recently, in 2000[34]. These compounds are all isostructural and have a structure based on infinite chains involving O···X-X···O units which are aligned along [-1 0 1] leading to an overall stoichiometry of $(C_4H_4O_2)\cdots X_2$.

Our aim was that by performing a high-resolution variable temperature neutron powder diffraction study we would be able to obtain accurate metric parameters for these complexes in addition to the lattice parameters. In particular, we were interested in potential variations in the inter O···X and intra X-X bond distances and any potential correlation between these two bond lengths. By also determining the thermal expansion properties of these compounds we would be able to ascertain the influence of changes at the atomic level on the macroscopic properties of the solid. From the accurate determination of hydrogen (deuterium) positions, the occurrence of any C-H···X hydrogen bonds could be unequivocally established. Study of the expansion properties on these systems (X_2 = Br_2, or I_2) we believed would enable us to observe which of these systems responded most readily to changes in temperature, and, coupled with the accurate structural information, would enable us to extract the features responsible for causing this behaviour, and hence, indirectly probe the nature of the O···X bond. Our overarching goal was by determining these components in the structure, would it be possible to tailor the expansion properties of these materials by a judicious choice of component molecules.

Experimental

Sample preparation and Data Collection

The preparation of these materials followed broadly the methods previously described in the literature [32,34]. Full details are given as electronic supplementary information.

For the neutron powder diffraction studies, the deuterated sample material was ground gently in an agate pestle and mortar cooled by immersion in a dry ice bath. The sample was then transferred into a thin-walled quartz-glass tube. Upon filling, the quartz-glass tube was placed in a thin-walled vanadium sample can. The can was then attached to a sample centre stick and then cooled to 4.2K in an AS “Orange” helium cryostat. High-resolution neutron powder diffraction patterns were then collected from this sample using the HRPD time-of-flight diffractometer at the ISIS facility of the STFC Rutherford Appleton Laboratory. For each of the samples, a series of short runs were collected as a

function of temperature whose primary purpose was to obtain accurate lattice parameters. These short runs were interspersed with longer runs to obtain accurate structural parameters in addition. However, the high quality of the samples coupled with the crystallographically imposed symmetry of the complex (point group 2/*m*, Z' = 0.25) was such that it was possible to obtain accurate structural parameters with a precision only marginally lower than the longer runs from the shorter data collection times.

Structure determination and refinement

Either literature structures or previously obtained single crystal structures were used as the starting models for the Rietveld profile refinement[35,36] of the neutron powder diffraction patterns. Data were used from the backscattering and 90º detector banks, which enabled data that covered the ranges 0.663 Å < d <. 3.846 Å (Br_2 complex) and 0.663 Å < d <. 3.892 Å (I_2 complex) to be used. It was possible to use a fully anisotropic model for the refinements on the Br_2 system, but in the case of the I_2 system, it was necessary to restrict anisotropic thermal parameters to the atoms of the dioxane molecule alone. It also was necessary to add a second phase to the refinement to account for the presence of weak Bragg peaks from the vanadium sample holder and cryostat windows and heat shields. In addition, it was observed that a small amount of residual dioxane was present for the sample containing Br_2 and this was added to the refinement using the known structure of the low temperature phase for 1,4 dioxane[37]. Rietveld plots showing observed calculated and difference patterns for the lowest temperature sets for each complex are shown in Figures 1 and 2. A summary of the refinements and selected crystallographic data are listed in Table 1 Crystallographic data have been deposited at the CCDC with deposition numbers CCDC 1904199-1904209 for 1904211-1904219 for $C_4H_8O_2Br_2$ and $C_4H_8O_2I_2$ respectively.

Results and discussion

Selected metrical parameters consisting of O···X, X-X and O···X-X bond lengths and angles for the bromine and iodine complexes are given in Table 2. Complete sets of bond lengths and angles are tabulated in supplementary data S1. Structural and packing diagrams for the complex are illustrated in Figures 3 - 6. The arrangements of the molecules within the unit cells is identical to that reported in the earlier x-ray structural determinations[32,34]. In general, there is some correspondence between the interatomic bond lengths and angles in the O···X-X fragments. For both compounds the O···X distances are significantly shorter than the sum of the van der Waals radii[38] and the X-X distances are longer than that observed for the free halogens in the gaseous phase as determined by spectroscopy; Br_2 2.2811 Å, I_2 2.6663 Å[39], and EXFAS I_2 2.681(2) Å[40]. In this last study EXAFS experiments were also performed in a series of solvents with the most pertinent I-I values being 2.694(3) Å in $(C_2H_5)_2O$ and

2.701(3) Å in C_2H_5OH. The distances are somewhat closer to those observed at comparable temperatures using neutron diffraction; Br_2 2.286(3)[41] Å, I_2 2.718(3) [42]. The elongation of the intramolecular halogen bond usually indicates the occurrence of a strong intermolecular halogen bond, with significant donor-acceptor interaction. Furthermore, for the case of the bromine compound, the differences between the interatomic contacts seen in the neutron-derived structure and the earlier x-ray structure are quite pronounced. For example at 136K the Br-Br and O-Br distances are 2.328(3) Å and 2.668(2) Å compared to the X-ray structure (temperature not stated) 2.31 Å and 2.71 Å[32]. These differences may be the result of the lower accuracy of the X-ray photographic investigation, or alternatively, the result of weakening of the halogen bond with increasing temperature (see below), or possibly a combination of both. In the case of the iodine complex the differences between our neutron I-I (2.7100(26) Å, I···O 2.7858(17) Å, and the previous x-ray study[34] I-I (2.693(1) Å I···O 2.808(3) Å) are far less pronounced, with the most noticeable differences being that in the X-ray study both the O···I distances and the I-I distances are shorter compared to our neutron study, though these differences are small. For both complexes, it can also be seen that there is a slight increase in O···I and O···Br distances with temperature, although these changes are small in absolute terms, and possibly statistically insignificant. In addition, in our investigation we find very little, if any, variation in the Br-Br and I-I distances with temperature. This is in marked contrast to earlier studies of the elemental halogens where there was a significant increase in intermolecular halogen contact distances with increasing temperature which is accompanied by a smaller decrease in the intramolecular halogen bond length[41,42]. In the case of the bromine complex, the distances we obtain at 4.2K are in good agreement with a theoretical study (MP2/6-311+G*) on this system[43]. Of greater interest is comparison of these current results with the contacts seen in the complex formed between acetone and bromine[22,30]. The Br-Br distances are found to be comparable; for the temperature range 4.2K -110 K the values lie between 2.326(2) Å - 2.341(2) Å in this current work, and are 2.321(3) Å and 2.328(3) Å in our earlier study[22,30] However, there are significant differences in the Br···O contacts which lie between 2.653(2) Å and 2.659(2) Å in this work and 2.734(2) Å and 2.737(2) Å for the distances in the acetone bromine system [22,30]. These longer O···Br distances are presumably the consequence of the carbonyl forming 2 halogen bonds, as opposed to one halogen bond in the dioxane complex.

For neither structure is the halogen situated in either a fully equatorial or axial site with respect to the ring (figure 3) but lies between these extremes. This can be observed in the torsion angles X··· O-C-D listed in Table 4, the moduli of whose values differ equally from the idealised values of mod 60. Fortuitously the electron density within 1,4 dioxane has been determined in a low temperature deformation study which showed the electron density around the oxygen due to the

non-bonding electrons to be arranged in “a kidney-shaped density”, rather than as “rabbit ears” seen intrans2,5-dichloro-1,4-dioxane[37]. Whilst the electron density is more diffuse in 1,4 –dioxane, it is still able to interact with the σ-hole on the halogen molecule.

In both crystal structures, the molecular structure, the bond lengths, angles and conformation of the dioxane molecules (lowest measured temperature) are very similar (C-C =1.4358(9) Å, C-O = 1.5206(16) Å) (Br_2) (C-C = 1.4347(11) Å, C-O = 1.5096(19) Å) (I_2) to the values seen in the low temperature deformation study (C-O = 1.4315(6) Å and 1.4294(6) Å C-C 1.5155(6) Å[37] This is in marked contrast to the complex formed between acetone and bromine, where there is a marked elongation of the C-O double bond of the carbonyl group. The absence of any perturbation of the donor dioxane molecule occurs despite the shorter O···X distances, and the X-X halogen distances which are comparable. Since the principal difference between the two donor molecules is the presence of π orbitals in acetone, the factors that are responsible for these differences, whilst difficult to associate unambiguously with a structural feature, would seem to some extent be correlated with the absence of π orbitals in dioxane.

In order to determine the thermal expansion properties (via the thermal expansion tensor) of the two compounds we have made use of the computer program PAScal[44,45]. At low temperatures there is significant deviation from linear behaviour of the linear and volume thermal expansion coefficients (supplementary data) and thus we have restricted the calculation of the linear thermal expansion coefficients to 50 K-136 K (Bromine) and 27 K –81 K (Iodine). Expansivity plots for both materials are shown in figure 3, together with two orientations for each compound. Information showing the magnitudes and directions of the principal axes of the thermal expansion tensor are shown in Table 3.

It can be clearly seen from the diagrams and Table 3 that the direction of minimum expansion in both complexes correlates with orientation of the chain axis of the molecules, i.e. along [-1 0 1]. This chain which is formed by the halogen molecules which form bridges between the dioxane molecules and constitute the strongest intermolecular interactions, the O···X halogen bonds. Since it would be expected that iodine would form stronger halogen bonds than bromine because of the deeper σ hole[46], we would expect to see smaller thermal expansion in the case of iodine molecule, which is indeed the case (Table 3). The largest linear thermal expansion for both compounds is along [0 1 0], whilst is difficult to unambiguously attribute the principal intermolecular forces operating in this direction, it is probable that they are dispersion forces associated with the respective halogens, rather than any possible C-D···O or C-D···X hydrogen bonds. Stronger dispersion forces would be

expected in the case of iodine as opposed to bromine leading to the smaller expansion coefficient in the case of iodine. Note that one principal axis is required to lie parallel to [010] for a monoclinic crystal with unique *b* axis (Neumann's law[47]). The expansion coefficient of intermediate magnitude is oriented slightly off the *c* axis for example in the Br_2 complex it lies approximately along [-1 0 5]. On viewing a packing diagram viewed along ***b*** it can be seen that this would correspond to an approximate rotation of the I_2 and dioxane molecule about the 2-fold axes running through the centres of each molecule. The principal intermolecular force opposing this rotation would be the halogen bond which would be expected to be stronger in the case of the iodine complex leading to a smaller expansion coefficient, which is observed experimentally.

In conclusion, our study shows that the distinct anisotropy of the thermal expansion of these compounds is caused by a clear variation in the strength of the intermolecular forces present in the complex. The greatest expansion is seen where the forces are most probably associated with dispersion forces associated with the halogen, with the greatest expansion being seen for the bromine complex. The other two forces involve interactions involving the sigma hole of the halogen. As a consequence of the larger and more positive sigma holes present in iodine as opposed to bromine, the attractive intermolecular forces will be greater in the former leading to a decrease in the the thermal expansion. The ability to associate the expansivity and magnitude with the forces present will in the long run enable the rational design of materials with tailored properties.

Conflicts of Interest

There are no conflicts of interest to declare"

Acknowledgments

We wish to thank STFC for provision of neutron beam time and consumables. We wish to acknowledge the contribution of our friend and colleague the late Dr W. G. (Bill) Marshall for his involvement in this work, and his significant contributions to the development of, and study of, molecular solids using neutron powder diffraction, especially at high pressure.

References

1 G. R. Desiraju, P. S. Ho, L., Kloo, A. C. Legon, R. Marquardt, P. Metrangolo, P. Politzer, G. Resnati and K. Rissanen, *Pure Appl. Chem.,* 2013, **85**, 1711-1713.

2 R. S. Mulliken, *J. Am. Chem. Soc.,* 1952, **74**, 811-824.

3 T. Brinck, J. S. Murray and P. Politzer, *Int. J. Quantum Chem*., 1992, **44**, **S19**, 57-64.

4 P. Politzer and J. S. Murray, *ChemPhysChem*., 2013, **14**, 278-294.

5 T Clark, M. Hennemann, J. S. Murray and P. Politzer, *J. Mol. Model*, 2007, **13**, 291-296.

6 P. Politzer, and J.S. Murray, *Theo. Chem. Acc,* 2012., **131**, 1114.

7 P. Politzer, K. E. Riley, F. A. Bulat and J. S. Murray, *Comp. & Theo. Chem*., 2012, **198**, 2-8.

8 P. Politzer, J. S. Murray and T. Clark Phys Chem, Chem, Phys. 2010, 12, 7748-7757.

9 P. Metrangolo, G. Resnati, T. Pilati and S. Biella, *Structure and bonding*, 2007, **126**, 105,-136.

10 R Bertani, P. Sgarbossa, A. Venzo, F. Lelj, M. Armati, G. Resnati, P. Metrangolo and G. Terraneo, *Coord. Chem. Rev*., 2010, **254**, 677-695.

11 K. Rissanen*, CrystEngComm*., 2008, **10**, 1107-1113.

12 P. Metrangolo and G. Resnati, *Science*, 2008, **321**, 918-919.

13 H. L. Nguyen, P. N. Horton, M. B. Hursthouse, A. C. Legon and D. W. Bruce, *J. Am. Chem. Soc*., 2004, **126**, 16-17.

14 C. M. Cho, X. Wang, J. J. Li, C. He, J. Xu, *Liquid Crystals*, 2013, **40**, 185-196.

15 L. J. McAllister, C. Präsang, J. *P-W* Wong, R. J. Thatcher, A. C. Whitwood, B. Donnio, P. B. Karadakov and D. W. Bruce, *Chem. Comun*., 2013, 3946-3948.

16 P. Auffinger, F. A., Hays, E. Westhof and P. S. Ho , *Proc Nat Acad Sci,* 2004**, 101**, 16789-16794.

17 V. Cody and P. Murray-Rust, *J. Mol Struct.*, 1984, **112**, 189-199.

18 G. Cavallo, P. Metrangolo, R. Milani, T. Pilati, A. Priimagi, G. Resnati and G. Terraneo, *Chem. Rev*., 2016, **116**, 2478-2601.

19 A Forni, P. Metrangolo, T. Pilati and G. Resnati, Crystal *Growth and Design*, 2004, **4**, 291-295.

20 K. M. Hutchins, K. A., Kummer, R. H. Groeneman, E. W. Reinheimer, M. A. Sinnwellm, D. C. Swenson and L. R. MacGillivray, *Crystengcomm*, 2016, **18**, 8354-8357.

21 R. H. Jones, K. S. Knight, W.G. Marshall, J. Clews, R. J. Darton, D. Pyatt, S. J. Coles and P, N. Horton, *Crystengcomm*, 2014, **16**, 237 -243.

22 W. G. Marshall, R. H. Jones and K. S. Knight S *CrystEngComm*, 2018,**20**, 3246-3250.

23 J.S.O. Evans, *J. Chem. Soc. Dalton Trans*., 1999, 3317 -3326.

24 D. A. Woodcock, P. Lightfoot, L. A. Villaescusa, M. J. Diaz-Cabanas, M. A. Cambloor and D. Engberg, *Chemistry of Materials*, 1999, **11**, 2508-2514.

25 B. K. Saha, J. *Indian Inst Sci*., 2017, **97**, 177-191.

26 K. S. Knight K. Shankland, W.I.F. David, N Shankland, and S. W. Love, Chem, Phys, Lett, 1996, 258, 490-494.

27 S. Crawford, M. T. Kirchner, D. Blaser, R. Boese, W. I. F. David, A. *Dawson, A. Gehrke,* R. M. Ibberson, W. G., Marshall S. Parsons and O. Yamamuro, *Angew. Chem. Int. Ed.,* 2009, **48**, 755- 757.

28 D. R. Allan, S. J. Clark, R. M. Ibberson, S. Parsons, C. R. Pulham, and L. Sawyer, *Chem., Commun.,* 1999, 751-752.

29 M. Prager, W. I. F. David and R. M. Ibberson, *J. Chem. Phys*., 1991, **95**, 2473-2480.

30 R. H. Jones, K. S. Knight, W. G. Marshall, S. J., Coles, P. N. Horton and M. B. Pitak, *Crystengcomm* 2013, 15, 8572. -8677.

31 W. G. Marshall, R. H. Jones, K. S. Knight, J. Clews, R. J. Darton, W. Miller, S. J. Coles and P. N. Horton, *Cystengcomm.* 2017, **19**, 5194-5201.

32 O. Hassel and J. Hvoslef, *Acta Chem Scand*., 1954, **8**, 873.

33 O. Hassel and K. O. Strømme, *Acta Chem Scand* ., 1959, **13**, 1775-1780.

34 H Bock and S. Holl, *Z. Naturforsch* 2001, **56b**, 111-121.

35 A. C. Larson and R. B. Von Dreele, "General Structure Analysis System (GSAS)", Los Alamos National Laboratory Report LAUR 86-748 2000.

36 B. Toby, *J. Appl. Cryst.*, 2001, **34**, 210 -213.

37 T. Koritanszky, M. K. Strumpel, J. Buschmann, P. Luger, N. K. Hansen and V. Pichonpesme. *J. Am. Chem. Soc*., 1991, **113**, 9148-9154.

38 R. Rowland and R. Taylor, *J. Phys. Chem*., 1996, **100**, 7384-7391.

39 D. A McQuarrie and J. D. Simon 1997 Physical Chemistry a Molecular approach 199 p 499 University Science Books. Saulasito, California, USA.

40 U. Buontempo, A. Di Cicco, M. Nardone, P. Postorino, A. Filipponi and M. Nardone, *J. Chem. Phys*., 1997, **107**, 5720-5726.

41 B. M. Powell, K. M. Heal, and B.H. Torrie, Molecular Physics, 1984, 53, 929-939.

42 R. M. Ibberson, O Moze, and C Petrillo, *Molecular Physics* 1992, 76, 395-403

43 R. Lo, A. Ballabh, A. Singh, P. Dastidar and B. Ganguly, CrystEngComm, 2012, 14, 1833-1841.

44 M. J. Cliffe and A. L. Goodwin, *J Appl Cryst*., 2012, **45**, 1321-1329.

45 M. J. Cliffe and A. L. Goodwin, *PASCal A web tool for Principal Axis Strain* ***Calculations*** http://pascal.chem.ox.ac.uk/.

46 M. H. Kolář, and P. Hobza, *Chem Rev*, 2016, **116**, 5155-5187.

47 F. E. Neumann 1885 *Vorlesungen über die Theorie der Elastizität der fester Körper und die Lichtäthers*. Edited O.E. Meyer, Teubner, Leipzig.

Table 1a

Unit cell parameters for complex formed between 1,4 dioxane and bromine Space Group *C*2/*m*

T/K	*a*/Å	*b*/Å	*c*/Å	β/º	V/Å^3	Rp	wRp	Chi^2	Np
4.2	9.55727(6)	8.92463(5)	4.1241(3)	90.372(1)	351.757(6)	0.0247	0.0251	5.100	94
50	9.56550(6)	8.93319(5)	4.1328(3)	90.479(1)	353.136(6)	0.0225	0.0223	4.054	92
59	9.56917(8)	8.93727(6)	4.1369(3)	90.521(1)	353.778(7)	0.0298	0.0281	1.884	92
68	9.57330(8)	8.94180(7)	4.1413(4)	90.565(1)	354.489(7)	0.0309	0.0294	2.050	92
78	9.57773(2)	8.94675(7)	4.1461(4)	90.610(1)	355.253(9)	0.0312	0.0290	2.004	92
88	9.58206(8)	8.95157(7)	4.1509(4)	90.658(1)	356.020(8)	0.0309	0.0284	1.929	92
102	9.58701(7)	8.95706(6)	4.1562(3)	90.708(1)	356.875(6)	0.0228	0.0223	4.226	92
110	9.59169(9)	8.96229(7)	4.1615(4)	90.757(1)	357.703(8)	0.0305	0.0279	1.869	92
118	9.59676(9)	8.96799(8)	4.1669(4)	90.806(1)	358.585(8)	0.0296	0.0272	1.774	92
126	9.60183(9)	8.97363(8)	4.1725(4)	90.858(1)	359.477(9)	0.0297	0.0272	1.772	92
136	9.60713(9)	8.979661(8)	4.17813(4)	90.912(1)	360.397(9)	0.0292	0.0264	1.659	92

Table 1b

Unit cell parameters for complex formed between 1,4 dioxane and iodine Space group *C*2/*m*

T/K	*a*/Å	*b*/Å	*c*/Å	β/º	V/Å^3	Rp	wRp	Chi^2	Np
4.2	10.1215(1)	9.2329(1)	4.30912(6)	90.286(1)	402.685(15)	0.0266	0.0241	4.321	85
7	10.1217(1)	9.2331(1)	4.30928(6)	90.285(1)	402.719(14)	0.0425	0.0378	1.357	83
17	10.1222(1)	9.2336(1)	4.31009(6)	90.274(1)	402.836(14)	0.0427	0.0374	1.317	83
28	10.1236(2)	9.2355(1)	4.31216(6)	90.254(1)	403.169(15)	0.0426	0.0379	1.339	83
37	10.1256(2)	9.2381(1)	4.31498(6)	90.229(1)	403.626(15)	0.0426	0.0372	1.342	83
50	10.1290(1)	9.2423(1)	4.31921(4)	90.190(1)	404.343(10)	0.026	0.0237	4.181	83
59	10.1325(1)	9.2466(1)	4.32334(5)	90.154(1)	405.058(13)	0.0334	0.0295	1.915	83
70	10.1370(1)	9.2521(1)	4.32854(5)	90.108(1)	405.968(14)	0.0337	0.0295	1.914	83
81	10.1413(1)	9.2572(1)	4.33323(5)	90.066(1)	406.804(14)	0.0328	0.0289	1.85	83

Table 2a

Selected interatomic contacts for complex formed between 1,4 dioxane and bromine

T/K	Br-Br/Å	O-Br/Å	O-C/Å	C-C/Å	C-D1/Å	C-D2/Å
4.2	2.326(2)	2.654(1)	1.4358(9)	1.5206(16)	1.0965(10)	1.0960(10)
50	2.325(2)	2.655(1)	1.4334(9)	1.5136(16)	1.0966(9)	1.0958(9)
59	2.328(2)	2.657(2)	1.4319(12)	1.5143(21)	1.0963(12)	1.0979(12)
68	2.337(2)	2.653(2)	1.4309(13)	1.5156(23)	1.0930(13)	1.0939(13)
78	2.334(2)	2.656(2)	1.4286(14)	1.5168(23)	1.0942(13)	1.0905(13)
88	2.341(2)	2.655(2)	1.4301(14)	1.5180(24)	1.0921(14)	1.0924(13)
102	2.338(2)	2.659(2)	1.4285(12)	1.5146(20)	1.0938(11	1.0946(11)
110	2.337(3)	2.659(2)	1.4287(15)	1.5134(27)	1.0921(14)	1.0916(14)
118	2.337(3)	2.659(2)	1.4278(15)	1.5127(27)	1.0917(15)	1.0912(14)
126	2.332(3)	2.666(2)	1.4251(16)	1.5141(29)	1.0914(15)	1.0905(15)
136	2.328(3)	2.668(2)	1.4262(16)	1.5089(30)	1.0908(16)	1.0921(15)

Table 2b

Selected interatomic contacts for complex formed between 1,4 dioxane and iodine

T/K	I-I/Å	I-O/Å	O-C/Å	C-C/Å	C-D1/Å	C-D2/Å
4.2	2.7100(26)	2.7858(17)	1.4347(11)	1.5096(19)	1.0992(12)	1.0971(13)
7	2.707(4)	2.7865(27)	1.4323(18)	1.5081(31)	1.0971(19)	1.0963(20)
17	2.710(4)	2.7878(27)	1.4315(18)	1.5114(31)	1.0971(19)	1.0946(20)
28	2.708(4)	2.7868(28)	1.4350(19)	1.5116(33)	1.0981(20)	1.0981(20)
37	2.708(4)	2.7961(29)	1.4324(19)	1.5101(35)	1.0953(20)	1.0956(22)
50	2.7052(28)	2.7930(19)	1.4338(13)	1.5064(23)	1.0995(14)	1.0944(14)
59	2.709(4)	2.7936(25)	1.4336(17)	1.5062(31)	1.0962(18)	1.0905(19)
70	2.710(4)	2.7985(27)	1.4315(18)	1.5030(32)	1.0945(19)	1.0921(20)
81	2.708(4)	2.7985(28)	1.4337(18)	1.4944(34)	1.0986(20)	1.0893(20)

Table 3a

Magnitude and direction of thermal expansion coefficients for complex formed between 1,4 dioxane and bromine for temperature range 50 -136K

			Direction		
Axes	$\sigma(MK^{-1})$	$\sigma\alpha(MK^{-1})$	***a***	***b***	***c***
X_1	29.6126	0.8811	0.6802	0	0.7330
X_2	59.5267	1.6121	0	-1	0
X_3	145.1079	6.1785	-0.1945	0	0.9809

Table 3b

Magnitude and direction of thermal expansion coefficients for complex formed between 1,4 dioxane and iodine for temperature range 27K - 81K

			Direction		
Axes	$\sigma(MK^{-1})$	$\sigma\alpha(MK^{-1})$	***a***	***b***	***c***
X_1	19.9734	1.0863	-0.7138	0	0.7004
X_2	44.9611	1.9250	0	-1	0
X_3	106.8475	3.4640	0.1768	0	0.9843

Table 4

Selected torsion angles for both complexes (4.2K structures)

X	X···O-C(1)-D(1)	X···O-C(1)-D(2)
Br	72.2	47.0
I	47.8	71.4

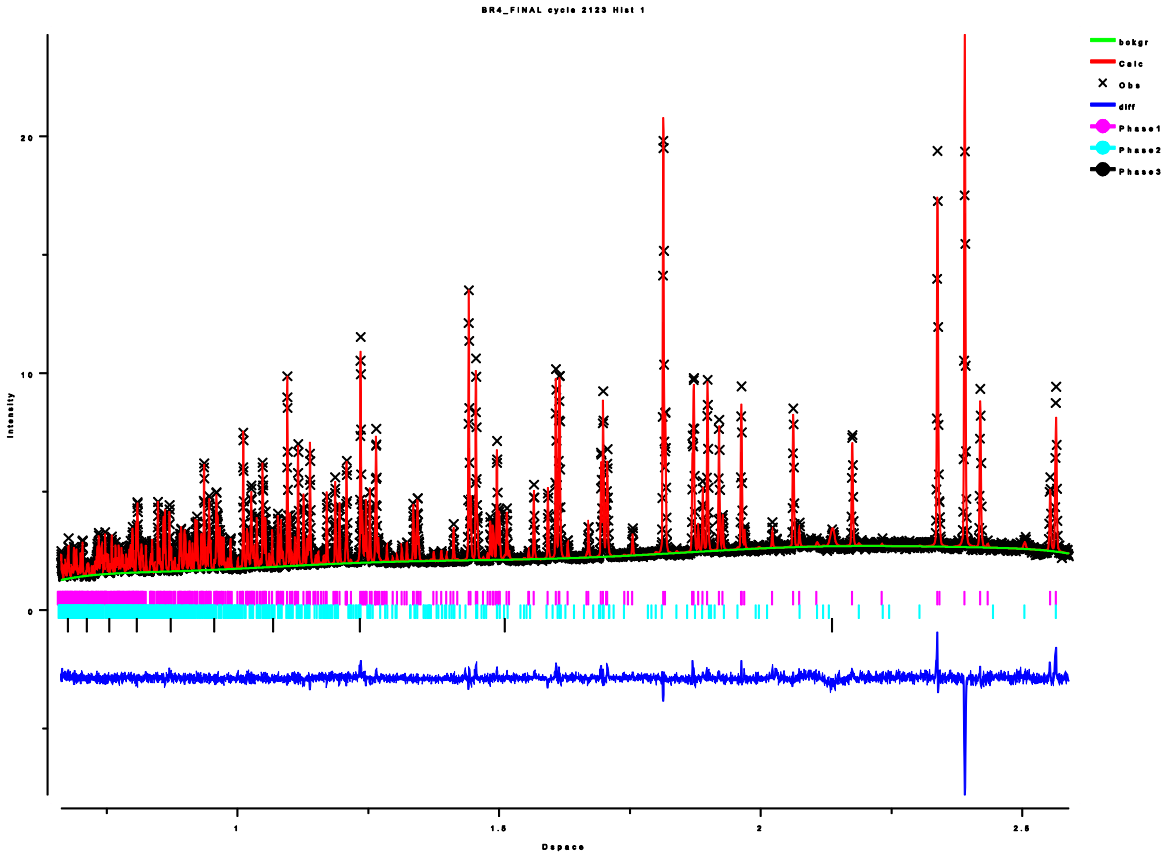

Figure1a Fitted neutron powder diffraction data from $C_4D_8O_2\cdots Br_2$ complex at 4.2 K collected in HRPD detector bank (<2θ> = 168.33º)

X = observed intensity, solid red calculated intensity, solid green background, solid blue difference, vertical pink lines reflection markers, complex, vertical turquoise lines 1,4 dioxane (phase II), vertical black lines vanadium.

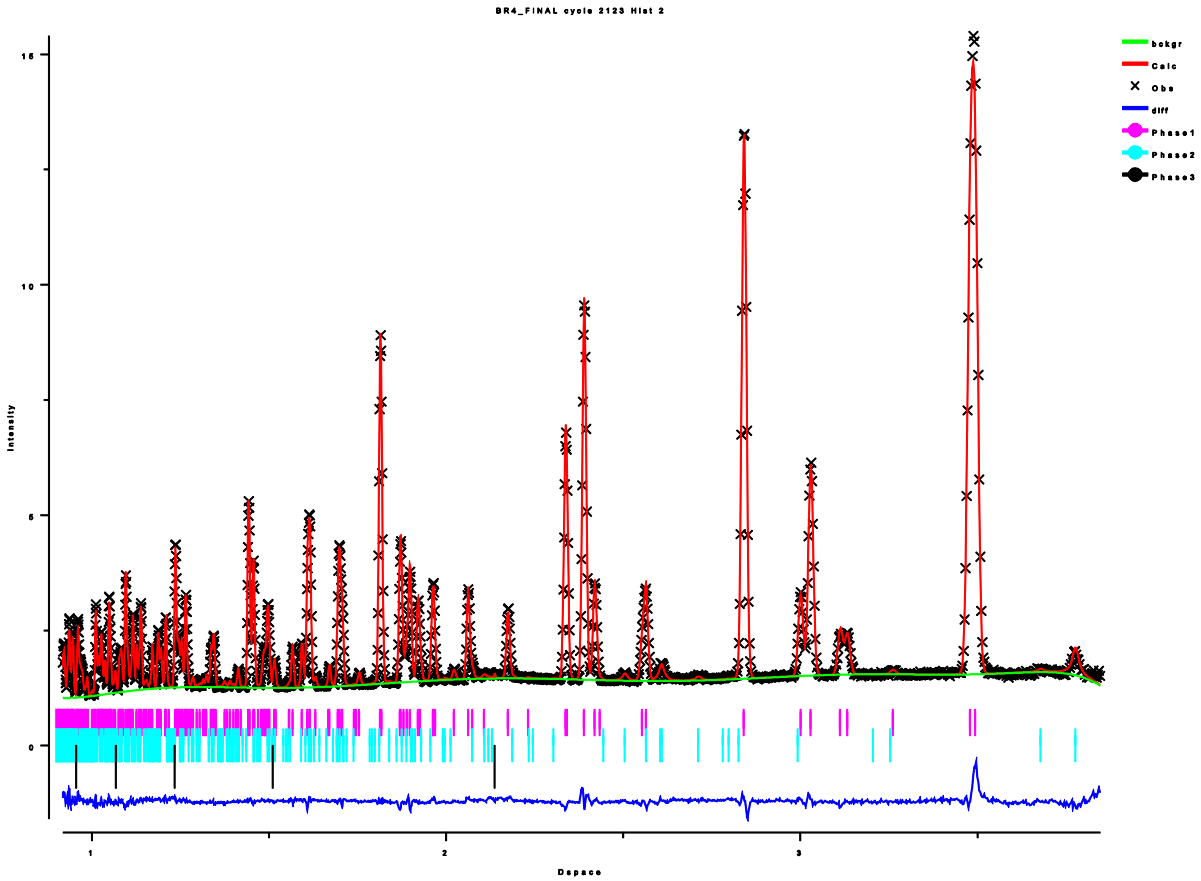

Figure1b Fitted neutron powder diffraction data from $C_4D_8O_2\cdots Br_2$ complex at 4.2 K collected in HRPD detector bank (<2θ> = 89.58°)

X = observed intensity, solid red calculated intensity, solid green background, solid blue difference, vertical pink lines reflection markers complex, vertical turquoise lines 1,4 dioxane (phase II), vertical black lines vanadium.

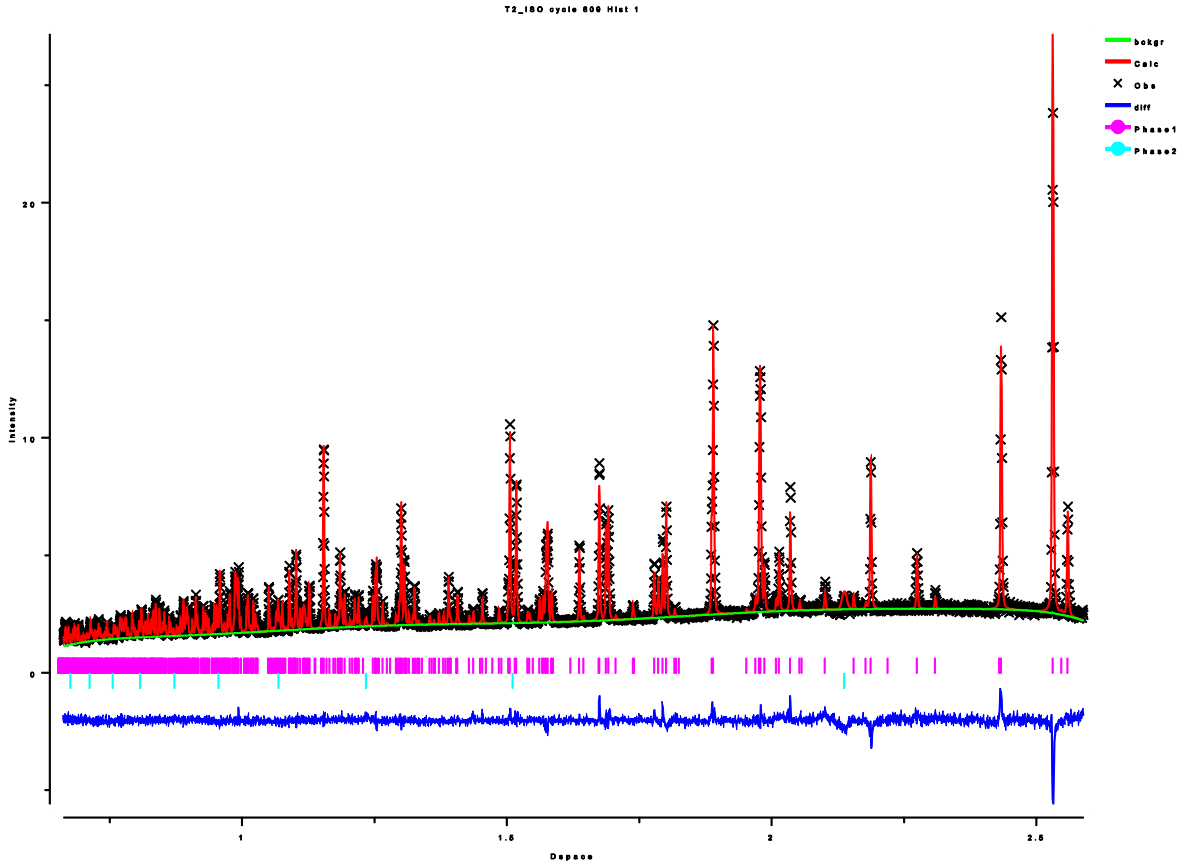

Figure2a Fitted neutron powder diffraction data from $C_4D_8O_2\cdots I_2$ complex at 4.2 K collected in HRPD detector bank (<2θ> = 168.33°)

X = observed intensity, solid red calculated intensity, solid green background, solid blue difference, vertical pink lines reflection markers, complex, vertical turquoise lines vanadium.

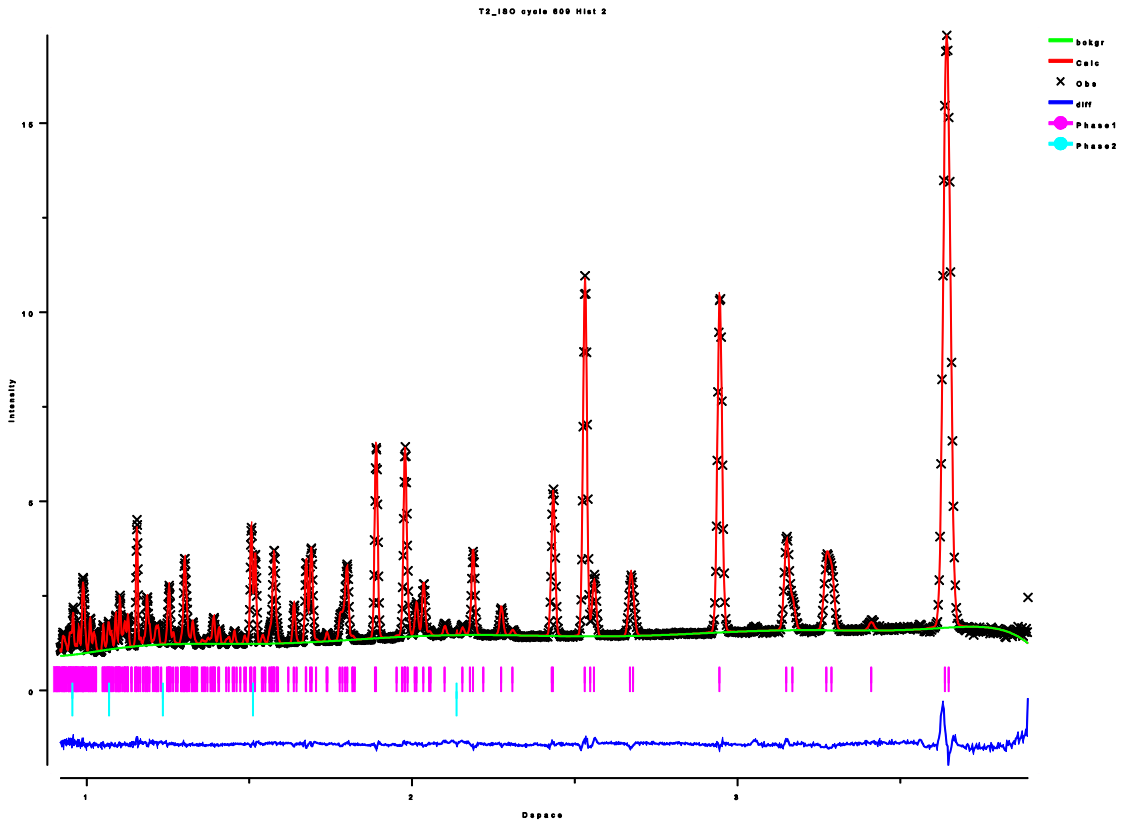

Figure2b Fitted neutron powder diffraction data from $C_4D_8O_2\cdots I_2$ complex at 4.2 K collected in HRPD detector bank (<2θ> = 89.58°)

X = observed intensity, solid red calculated intensity, solid green background, solid blue difference, vertical pink lines reflection markers complex, vertical turquoise lines vanadium.

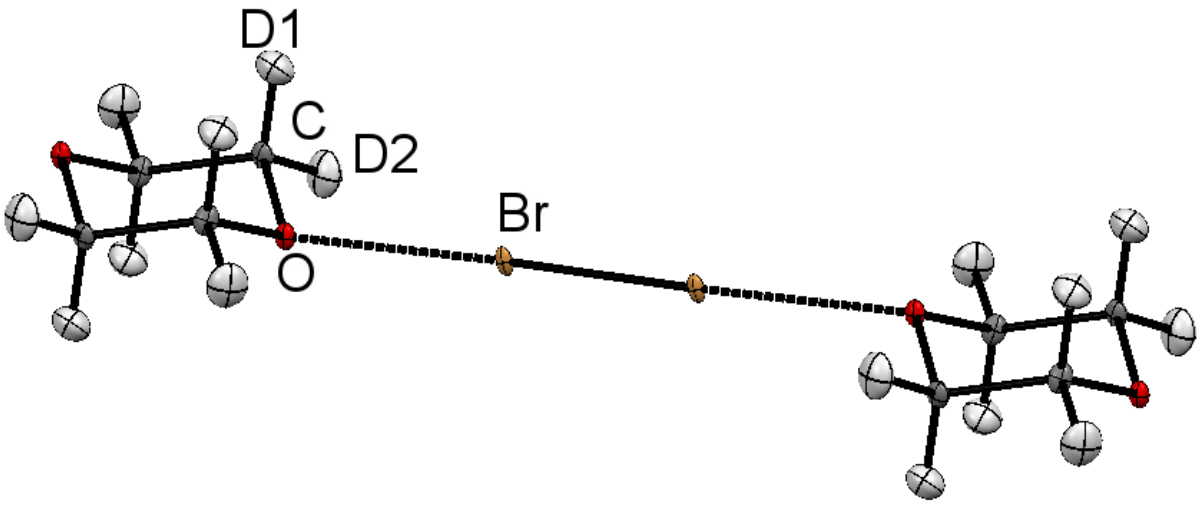

Figure 3a Structural diagram of the $C_4D_8O_2\cdots Br_2$ complex (4.2K) Thermal ellispoids drawn at 50% probability.

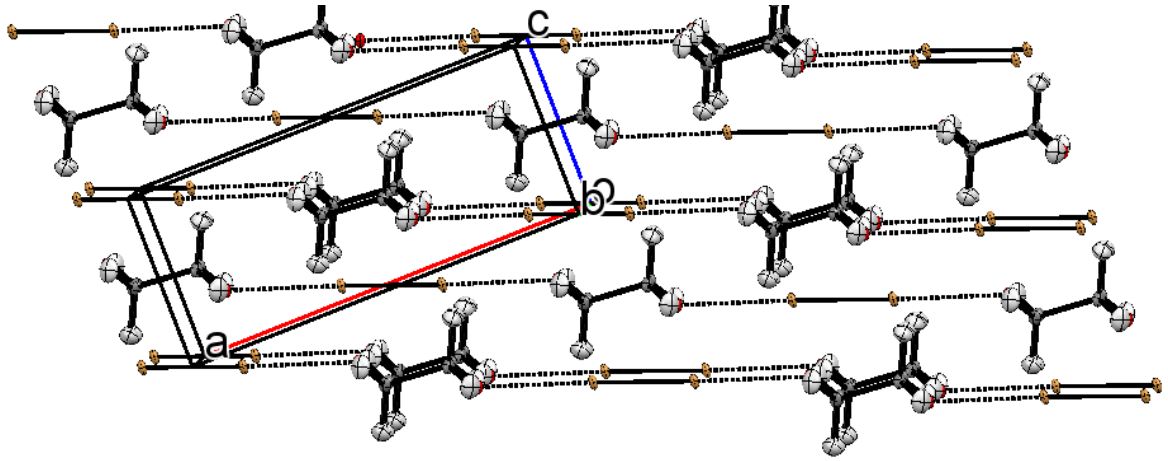

Figure 3b packing diagram of the $C_4D_8O_2\cdots Br_2$ complex (4.2K)

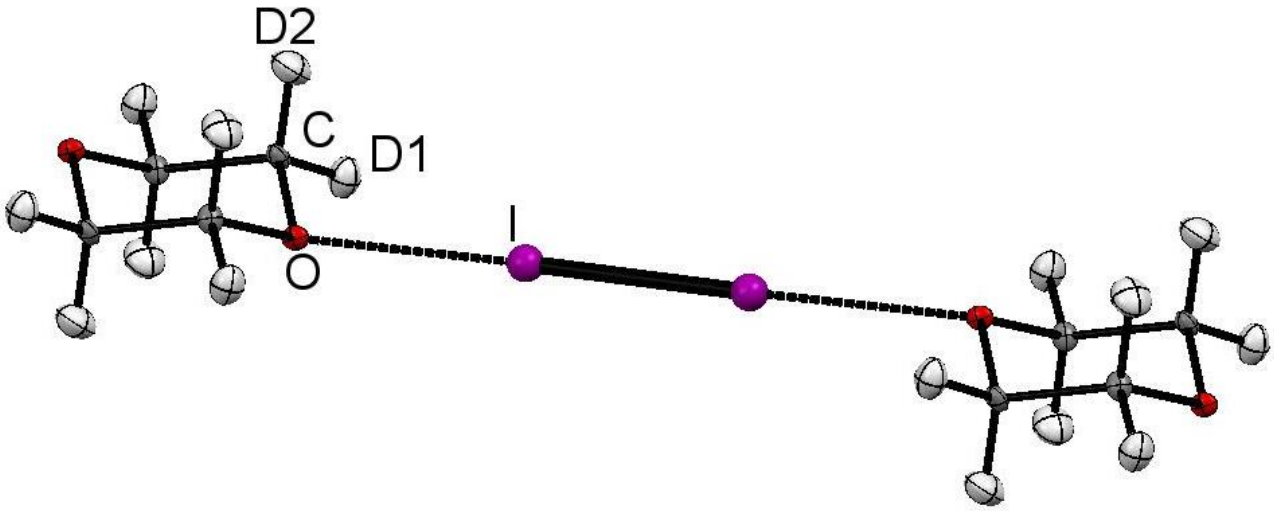

Figure 3c Structural diagram of the $C_4D_8O_2\cdots I_2$ complex. Thermal ellispoids drawn at 50% probability.
Iodine atoms drawn at arbirary radius
I

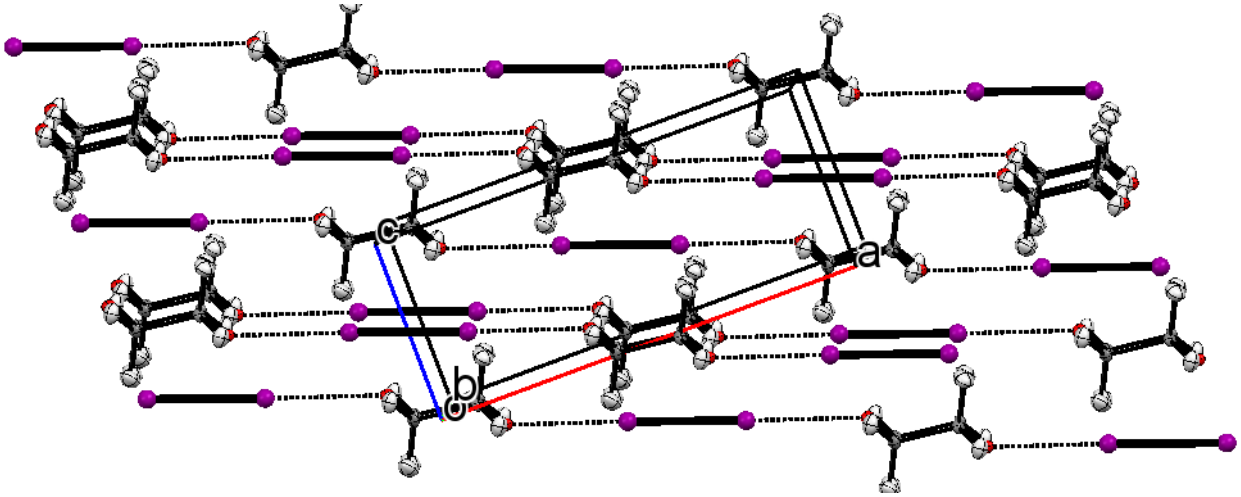

Figure 3d packing diagram of the $C_4D_8O_2\cdots I_2$ complex, Thermal ellispoids drawn at 50% probability. Iodine atoms drawn at arbirary radius

I

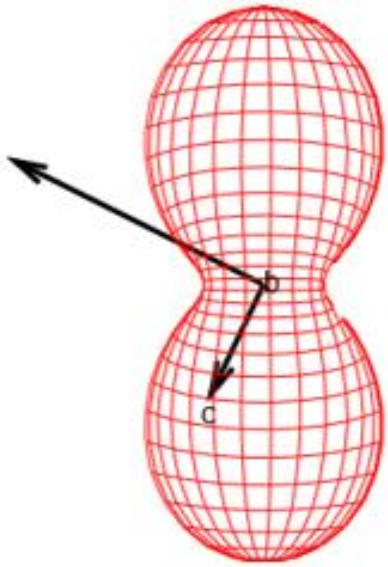

(i)

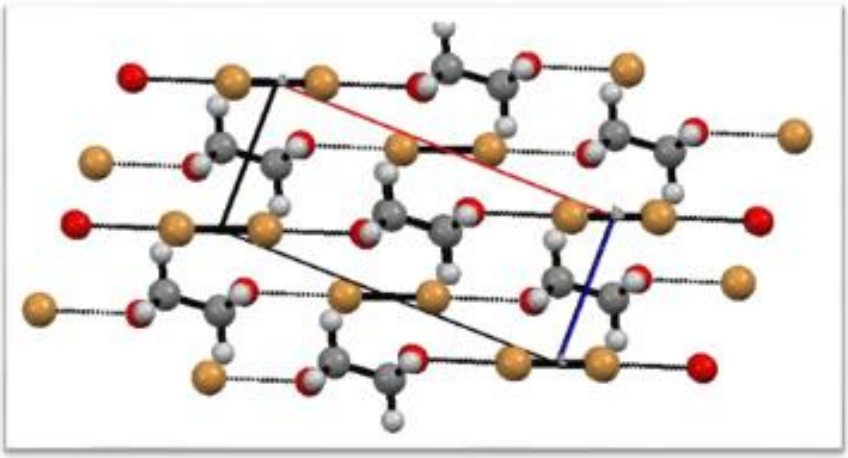

(ii)

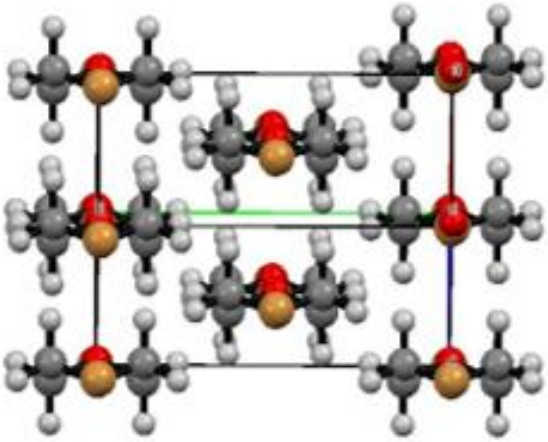

(iii)

Figure 4a Thermal expansivity plot (50 – 136 K) (i) and view of packing down b (ii) and rotation of b by 90 ° (iii) for the complex formed between 1,4 dioxane and bromine.

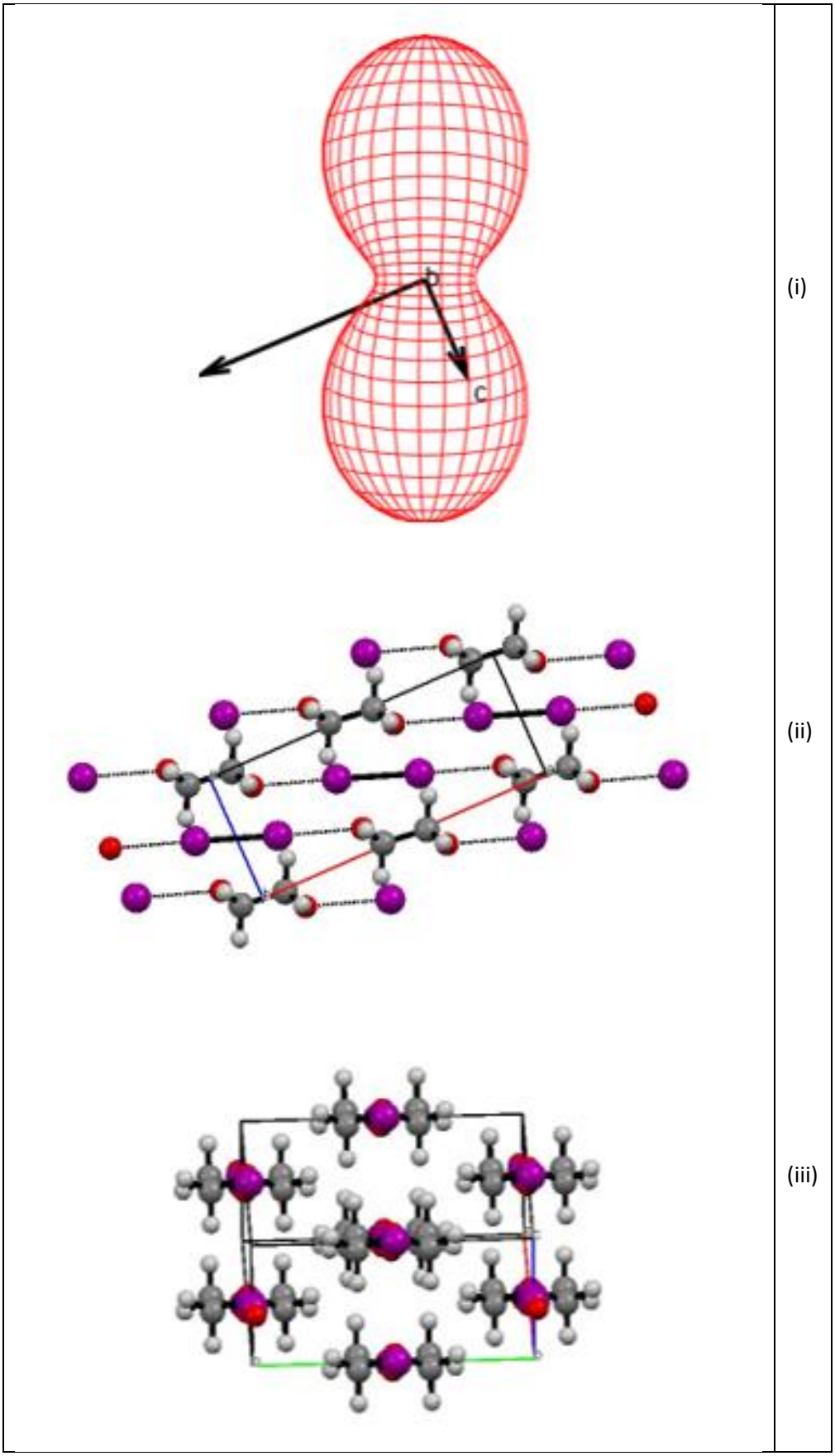

Figure 4a Thermal expansivity plot (27K 81K) (i) and view of packing down b (ii) and rotation of b by 90 ᵖ (iii) for the complex formed between 1,4 dioxane and iodine.